Schiller, A., Schattauer, I. and Ottowitz, D., 2016. Advanced data processing of airborne electromagnetic data for imaging hidden conduit networks in the coastal karst plain of Tulum (Mexico). *Boletín Geológico y Minero*, 127 (1): 7-19
ISSN: 0366-0176

Advanced data processing of airborne electromagnetic data for imaging hidden conduit networks in the coastal karst plain of Tulum (Mexico)

A. Schiller[(1)], I. Schattauer[(1)] and D. Ottowitz[(1)]

(1) Geological Survey of Austria, Vienna, Austria.
Geologische Bundesanstalt Neulinggasse 38, 1030 Wien.
Arnulf.Schiller@geologie.ac.at

ABSTRACT

This study is part of a series of international research cooperations which commenced in 2007 and are still ongoing. The study area is located on the east coast of the Yucatan Peninsula, Mexico, and comprises the northern most part of the Sian Ka'an biosphere reserve, a coastal wetland of international importance, as well as the city of Tulum in the state of Quintana Roo, and part of the second largest barrier reef in the world some 300 metres to one kilometre off shore. Two airborne surveys, conducted in 2007 and 2008 by the Geological Survey of Austria, covered an area of some 200 square kilometres, including the well-known Ox Bel Ha cave system, already mapped by exploration divers. In order to get additional ground truth data and input for the hydrological model, extended ground geophysical campaigns have been conducted annually. The first processing of the airborne electromagnetic (AEM) data revealed not only a clear signature from known caves but also the image of a vast, unexplored, hidden conduit network. However, lateral and depth resolution was limited due to measurement drift and noise as well the specific behaviour of the applied inversion technique. Newly developed algorithms for processing AEM data and inversion results have improved the signal-to-noise ratio significantly and enabled the imaging of well defined structures in the underground. Therefore, the AEM method is now capable of quickly deliver crucial structural information of karst-water regimes in difficult accessible areas with unique depth information compared to previous studies.

Key words: airborne electromagnetics, conduit network, karst ground-water modelling.

Técnicas avanzadas de análisis de datos electromagnéticos aerotransportados para cartografía de redes de conductos kársticos de la planicie costera de Tulum (México)

RESUMEN

El presente trabajo es el resultado de la colaboración internacional en investigación que comenzó en 2007 y que todavía continúa. El área de estudio se encuentra en la Península de Yucatan (México) y comprende el extremo norte de la reserva de la biósfera de Sian Ka'an, la población de Tulum en el estado de Quintana Roo, y parte del segundo arrecife de barrera más grande del mundo y que se encuentra a entre 300 y 1000 m de la playa. Se realizaron dos campañas aerotransportadas, en los años 2007 y 2008, por el Servicio Geológico de Austria, cubriendo un área de unos 200 km², y que incluyó el bien conocido sistema kárstico Ox Bel Ha, que ya había sido cartografiado mediante espeleobuceo. A fin de contar con más datos de campo para verificación y para entrada al modelo hidrológico, se han llevado a cabo campañas anuales de prospección geofísica en superficie. El primer procesado de los datos electromagnéticos aerotransportados reveló no solo una fuerte señal de las cuevas ya conocidas, sino también la existencia de una extensa red de conductos kársticos desconocidos anteriormente y por lo tanto todavía inexplorados. Sin embargo, la

resolución lateral y en profundidad fue limitada debido al ruido y deriva de la medición; así como por las características específicas de la técnica de inversión aplicada. Como resultado de esta investigación se desarrollaron nuevos algoritmos para un postproceso cuidadoso de los datos electromagnéticos aerotransportados e inversión de los resultados que permiten mejorar significativamente la relación señal/ruido y posibilitan la cartografía detallada de las estructuras subterráneas. Finalmente se concluye que el método de mediciones electromagnéticas aerotransportadas es ahora un método capaz de proveer rápidamente de información sobre la estructura de sistemas kársticos y su funcionamiento hidrológico para áreas de difícil acceso; así como información en profundidad única si se compara con resultados previos.

Palabras clave: electronagnetismo aerotransportado, red de conductos, modelo de aguas suberráneas kársticas.

VERSIÓN ABREVIADA EN CASTELLANO

Introducción

Los acuíferos kársticos representan importantes, pero vulnerables, fuentes de abastecimiento de agua a una parte significativa de la población de la Tierra. Para el uso sostenible de estos recursos es necesario el desarrollo de herramientas de gestión integrada basadas en modelos numéricos del agua subterránea. El estudio presentado en este artículo es parte de una serie de cooperaciones internacionales de investigación, iniciadas en el año 2006 y todavía en curso, que tienen la intención común de desarrollar y probar métodos innovadores de adquisición de datos y métodos de modelización para proporcionar dichas herramientas en un contexto socio-económico-ecológico de gran actualidad. El área de estudio se encuentra en la península de Yucatán (México) y comprende la parte más al norte de la Reserva de la Biosfera (UNESCO)de Sian Ka'an, un humedal costero de importancia internacional, así como el pueblo de Tulum, Quintana Roo y parte de la segunda barrera arrecifal que se encuentra a entre unos 300 metros y un kilómetro de la costa (Fig. 1). En el subsuelo, y por debajo de la ciudad, toda la zona está atravesada por una vasta red de cuevas submarinas. La capa superior del acuífero kárstico, de agua dulce, representa en realidad el único recurso de agua subterránea para la región. Sin embargo este recurso está en peligro por el rápido desarrollo urbano y la insuficiente gestión de las aguas residuales. Además, la contaminación del agua subterránea también podría amenazar la bioreserva Sian Ka'an, situada a unos pocos kilómetros al sur de Tulum. En este contexto, la gestión sostenible del agua, así como la protección de los arrecifes y la bioreserva requiere de una mejor comprensión del régimen del agua kárstica y de su dinámica. En principio, los acuíferos kársticos se caracterizan por la presencia de dos dominios de flujo diferenciados: la matriz de roca caliza y los conductos kársticos. Un modelo de flujo de acuíferos kársticos requiere información espacial detallada sobre las características de los dos dominios. Los métodos electromagnéticos de determinación de la distribución de la resistividad eléctrica dentro del subsuelo podrían proporcionar dicha información (Reynolds, 1997). Para explorar la aplicabilidad del electromagnetismo aerotransportado, se realizaron dos campañas en 2007 y 2008 por el Servicio Geológico de Austria, cubriendo un área de unos 200 kilómetros cuadrados en total (Fig. 2, Supper et al., 2009).

Metodología

El sistema de medición austríaco consiste en una sonda electromagnética remolcada 30 metros por debajo de un helicóptero, incluyendo el suministro de potencia y el cableado para transmisión de datos (Motschka, 2001). La sonda se vuela aproximadamente a 50 metros por encima del suelo y a una velocidad de 120-150 km/h. Cuatro bobinas transmiten un campo electromagnético en cuatro canales de frecuencia (0.4 kHz, 3.2 kHz, 7.6 kHz y 28.8 kHz) que induce corrientes torbellino en el subsuelo. Cuatro bobinas receptoras, que también van montadas en la sonda, miden la amplitud y la fase de los campos secundarios irradiados desde estas corrientes torbellino. La inversión de los datos medidos proporciona la distribución de la conductividad eléctrica aparente hasta profundidades máximas de 150 metros. El procesado estándar inicial de datos electromagnéticos aerotransportados reveló una firma clara de cuevas ya conocidas, pero además proporcionó la imagen de una vasta red de conductos kársticos ocultos y desconocidos con anterioridad. Sin embargo, la resolución lateral y en profundidad es limitada debido a la deriva en las medidas y relativamente mal ratio señal/ruido, así como limitaciones propias de la técnica de inversión aplicada (Supper et al., 2009). El análisis cuidadoso de la deriva y ruido inmanentes del sistema, así como la identificación de sus fuentes (Schiller et al., 2010), posibilitaron el desarrollo de técnicas novedosas de postproceso para la reducción del ruido y de la deriva, así como la obtención de imágenes de información estructural del subsuelo a través de proceso avanzado de los resultados estándar de la inversión.

Proceso de datos

En el caso de la prospección electromagnética aerotransportada (AEM) de Tulum se han aplicado los procedimientos siguientes:

- *Reducción general del ruido gausiano (estándar).*
- *Escalado de la Q-bobina (estándar).*
- *Reducción de la deriva lineal mediante la anulación de datos (estándar).*
- *Amortiguación de interferencias activas externas (avanzado).*
- *'Anular en línea': estimación automática de la deriva y corrección con datos de altitud (corrección de deriva del transmisor, receptor y estimación de la deriva residual - avanzado).*
- *'Método del gradiente sintético': estimación del desplazamiento de la deriva residual mediante el análisis de la correlación de altitud y su corrección (avanzado).*
- *Edición semiautomática de datos (estándar).*
- *Mejora de las estructuras lineales (avanzado).*
- *Inversión de datos (estándar).*
- *Reducción de fondo para la mejora de la información estructural (avanzado).*

La corrección automática de la deriva funciona con datos recogidos a altitudes por encima de un cierto límite, ajustable y dependiente de la región (por ejemplo, 200 m en Tulum). En altitudes superiores a este límite se supone que no se detecta ninguna señal más del suelo, por lo que la amplitud restante es causada por la deriva. Muy a menudo la topografía es del tipo que el límite de altitud se alcanza también durante la medición por lo que se puede utilizar la información para la estimación más precisa de la deriva y la corrección (Fig. 4). Otra forma para estimar la deriva residual es el análisis de la correlación señal-altura. Ésta utiliza el hecho de que, en general, la señal bruta exhibe una fuerte correlación con la altura de medición. Extrapolando la dependencia de la altura de los datos de la señal dentro de una cierta ventana a altitud infinita se obtiene el desplazamiento residual que representa la deriva ("método del gradiente sintético", Fig. 5). Después de la corrección de la deriva y una revisión final y edición ocasional de artefactos residuales, los datos pueden ser transformados a una altura constante sobre el suelo y filtrados. Para realzar las estructuras lineales se ha desarrollado una novedosa técnica de procesamiento de imágenes. Aquí se utiliza un filtro lineal de promedio ponderado que se pone en cada punto del mapa y las salidas se calculan para rotación del filtro de 180°. La salida máxima se almacena en una nueva imagen. La técnica se resume en la figura 7; la entrada y la salida se muestran en las figuras 6 y 8. Este filtro proporciona un mapa con mejor ratio señal/ruido y con estructuras claramente visibles que indican posibles conductos. Sin embargo, el mapa no contiene información de profundidad. La inversión de profundidad del dominio de la frecuencia de datos EM considera la penetración en el suelo, dependiente de la frecuencia (profundidad de la zona superficial), de un campo electromagnético - a frecuencia más baja más profunda es la penetración-. Así, cada medición (10 por segundo) es tratada como un sondeo electromagnético de profundidad basado en cuatro canales de frecuencias. Se calcula un modelo 1D de la resistividad eléctrica de capas del subsuelo para cada posición de la prospección. Para estos cálculos se aplicó el software UBC EM1DFM 1.0, desarrollado en la University of British Columbia. Durante la inversión, se modificó la resistividad eléctrica de hasta 25 capas con espesores variables, para poder ajustar los datos experimentales de AEM. Los resultados de inversión usuales -es decir, la sección de profundidad debajo de una línea de prospección- muestran mínimos y máximos de la distribución de conductividad eléctrica similar a una cadena de montañas donde los picos se correlacionan con los conductos, pero no son visibles estructuras bien definidas. El análisis detallado demostró que un gran gradiente vertical está dominando el resultado de la inversión que es causado por el fuerte campo secundario originado por el cuerpo de agua salada. La idea era que este fuerte gradiente podría ocultar señales más débiles correlacionadas con información estructural. En consecuencia, el campo fue modelado y sustraído de la inversión inicial para realzar la información estructural oculta (Figs. 10, 11).

Resultados y Conclusiones

Las técnicas de corrección automática de deriva permiten ahorrar tiempo y tienen en cuenta también la deriva del transmisor, así como parte de la deriva del receptor. En los casos de estudio de topografías abruptas, los procedimientos convencionales de "nulling" podrían ser sustituidas por "in-line nulling" lo que ahorra tiempo y combustible. El método del gradiente sintético reduce la mayor parte de la deriva residual si la calidad de los datos y la disposición geológica son favorables. El procesamiento del filtro rotativo mejora significativamente la relación señal a ruido y produce una definición lateral de estructuras muy buena (también puede acentuarse una orientación preferente). La reducción de fondo de los resultados de inversión estándar proporciona la información más legible, tanto lateral como en profundidad, de estructuras kársticas

capturadas por AEM hasta la fecha. Las estructuras se correlacionan generalmente bien con conductos conocidos (Fig. 12). Diferentes técnicas de modelado de fondo se podrán analizar en un futuro próximo para extraer información sobre la superficie freática y la haloclina en las aguas subterráneas del karst. En un siguiente paso se pretende la elaboración de un modelo 3D de la red de conductos. Sin embargo, esto requiere una preparación muy cuidadosa de los datos, que está actualmente en curso. Con estos estudios aerogeofísicos se demostró sus ventajas en estudios hidrológicos, es decir, la rápida obtención de información estructural fundamental en un sistema kárstico en un área de difícil acceso. El procesado avanzado de datos mejoró significativamente la información en profundidad hasta 50 m o más. Mientras que el contexto de este estudio se refiere específicamente a las posibles repercusiones de la urbanización en curso en el área de Tulum sobre los recursos hídricos kársticos, los métodos aplicados desarrollan también contribuciones importantes en estudios similares de agua subterránea y en entornos más complejos, como por ejemplo los que se encuentran en el entorno del mar Mediterráneo.

Introduction

Karst aquifers represent important but vulnerable sources for water supply to a significant part of the earth's population. For sustainable use of these resources, development of integrated management tools based upon numerical groundwater models is required. This study is part of a series of international research cooperations which commenced in 2006 and are still ongoing and have the general intention of developing and testing innovative data acquisition and modelling methods for providing such tools within a highly topical socio-economic and ecologic context such as those found in the area of Tulum, Quintana Roo. Here, the Sian Ka'an UNESCO world heritage biosphere reserve, a coastal wetland of international importance, as well as the growing town of Tulum, and part of the second largest barrier reef in the world meet. In the subsurface, and below the city, the whole area is connected by a vast network of underwater caves. The cave systems are world famous for their extension and clear water. Up to 1000 km of surveyed caves have been reported in the exploration divers' community. The topmost, or fresh-water layer of this groundwater regime actually represents the only fresh-water resource of the region, apart from the higher lagoons of the bio reserve which are protected. This important resource is endangered by rapid urban development and insufficient plans for a sustainable water management. Furthermore, the situation is critical because outlets of the conduit network are located within the second largest barrier reef system of the world. Ground-water contamination could also threaten the Sian Ka'an bio-reserve, located only a few kilometres south of Tulum. In this context, both sustainable water management and the protection of the reef and the bio reserve require a better understanding of the karst-water regime, its potential and its dynamics. Important studies are given in Beddows, 2004, Gondwe *et al.* 2010a and 2010b, or Bauer-Gottwein *et al.* 2011. However, the research is complex due to the limited accessibility of the system which is only possible through cenotes, widely distributed over the bush plane, a few wells or through bore holes (Supper *et al.,* 2010). Hence, one of the goals was to assess the applicability of airborne geophysics for acquiring hydrologically relevant data which has the advantage of rapid, comfortable scanning of the underground over wide and difficult terrains with a helicopter-borne measurement system. Airborne electromagnetics (AEM) was especially tested since it measures the electrical conductivity distribution in the underground which correlates with water saturation and porosity (Reynolds, 1997).

After initial ground geophysical surveys with promising results, two airborne campaigns took place in 2007 and 2008 (Supper *et al.,* 2009, Ottowitz, 2009). The AEM method was especially useful as it revealed a first rough picture of underground structures, which correlated with systems already surveyed by exploration divers and a general halocline surface could also be interpreted. This structural information was later incorporated into a statistical karst-network simulation and a preliminary groundwater model (Vuilleumier, 2011). However, the picture was still blurred by immanent measurement noise and drift which degrades high resolution lateral and depth information. As a consequence, detailed analysis of noise and drift has been conducted (Schiller *et al.,* 2010). Based upon the results of these analyses advanced AEM data processing methods have been developed which improve the results significantly. The improved AEM imaging shows unprecedented depth resolution and correlates well with known karst structures.

Survey area

The survey addresses the coastal karst plain containing the town of Tulum, which is mainly covered

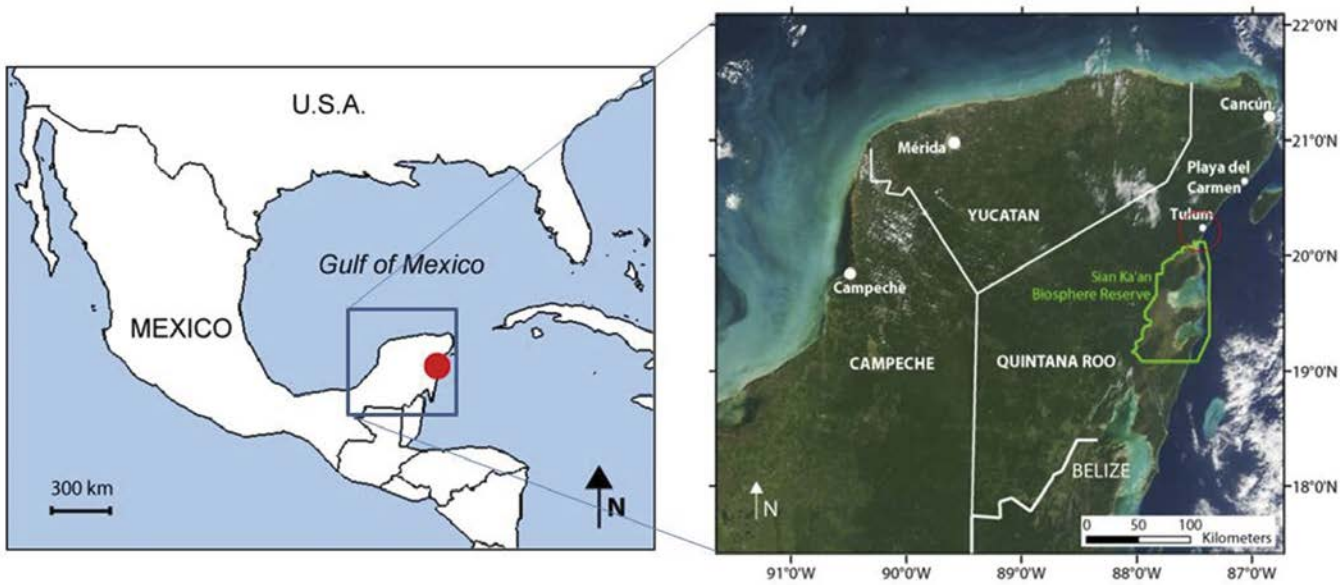

Figure 1: Location of the survey area (red) and the Sian Ka'an biosphere reserve (green).
Figura. 1*. Localización del área de estudio (rojo) y de la Reserva de la Biosfera de Sian Ka'an (verde).*

with bush and exibits flat topography (Fig. 1). The conduit network the study focuses on developed in nearly horizontal layered limestone predominantly during ice ages when the sea level was up to 100 metres lower. The limestone reaches depths of several thousand metres and exhibits varying porosity, spanning from very compact to very permeable, typical for young reef limestone. The caves or conduits seem to be concentrated mainly in the top 40 metres. However, in some places there is indication of deeper systems with maximum depths of around 100 metres (Beddows, 2004). The thickness of the fresh-water layer spans from zero at the coast to some 15 to 30 metres, with distances from the coast increasing to 25 kilometres. Below the fresh-water layer there is salt water intruding from the sea and reaching deeper regions. The network is constrained inland to the north east by the Hol Box fracture zone. Further inland there are isolated cenotes with some shorter connected tunnels but no other network is known with comparable extent and complexity. Known outlets of the conduit network are located in the lagoons of the bio-reserve and between the beach and the barrier reef (Beddows, 2004).

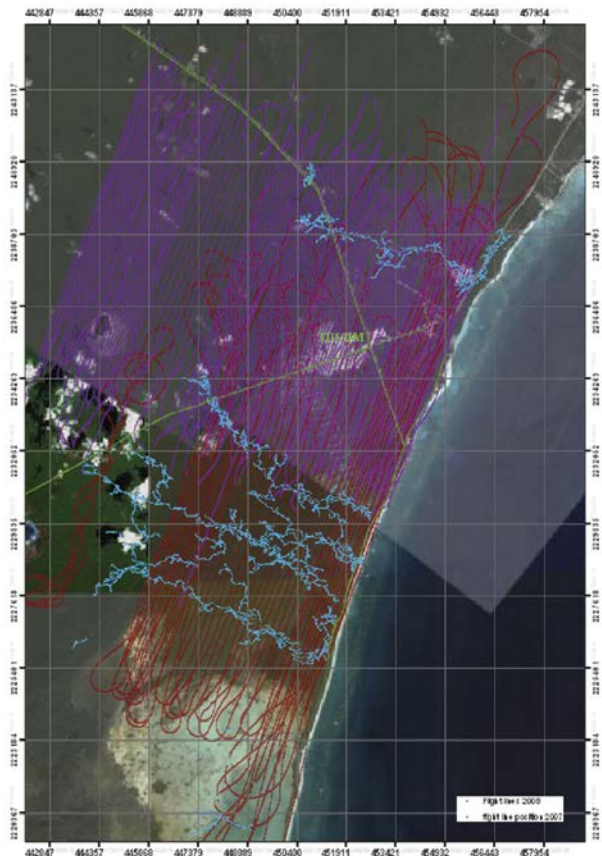

Figure 2: Location of flight lines and of explored branches of the cave systems Ox Bel Ha, Ich Tunich and Sac Actun.
Figura 2*. Localización de las líneas de vuelo y de las partes exploradas de los sistemas de cuevas Ox Bel Ha, Ich Tunich y Sac Actun.*

Objectives

In principle, karst aquifers are characterized by the presence of two distinct flow domains: the limestone matrix and the karst conduits. A flow model of karst

aquifers requires detailed, spatially distributed information on the characteristics of the two domains. Methods which determine the distribution of the electrical resistivity within the subsurface may provide innovative input information to improve groundwater modelling of karst aquifers. To explore the potential of airborne electromagnetics (AEM) for achieving this, two airborne surveys were carried out in 2007 and 2008, covering an area of some 200 square kilometres in total (Fig. 2). Initial results were produced by standard data processing techniques (Supper *et al.,* 2009). While a general picture of the conduits was achieved there was still a high noise level present in the data which avoided the resolution of finer details or depth defined structures.Therefore, one objective was to study the mechanisms responsible for blurring the picture and to develop methods for improving signal-to-noise ratio as well as depth resolution.

Methods

Measurement principle

The measurement device is a torpedo-like electromagnetic frequency domain probe ('bird'), towed 30 metres below a helicopter with power and data cabling (Motschka, 2001). The probe is dragged approximately 50 metres above ground at 120-150 km/h. Four transmitter coils (two coplanar, two coaxial), mounted in the head section of the bird transmit an electromagnetic field in four frequency channels (0.4 kHz, 3.2 kHz, 7.6 kHz and 28.8 kHz) which induces eddy currents in the subsurface. Four receiver coils (two coplanar, two coaxial) are mounted in the bird's rear section with a separation of approximately four metres between the transmitter and the receiver coils. The receiver coils measure amplitude and phase of the sum of secondary field radiating from these eddy currents in the ground as well as the primary field radiating from the transmitter coils. To cancel out the primary field bucking, coils with less turns are mounted near the transmitter and connected serially with inverse polarity to the receiver coils. If adjusted optimally, practically all the pure secondary field originating in the subsurface is left. This secondary field is referred to as the primary field with amplitude in parts per million (ppm) of the primary field strength and with phase difference. An equivalent representation is the in-phase and quadrature component of the measurement signal. The standard measurement is conducted ten times per second, which corresponds to a spacing of about three metres in mean. Typical of frequency-domain systems is significant non-linear signal drift which we tried to minimize through nulling of the signal in higher altitude above ground (1000 feet). At these altitudes no more secondary field is expected to originate from the ground due to an exponential decay with height. The drift between nulling phases is then linearly fitted and substracted. However, a lot of non-linear drift remains. Gaussian noise levels

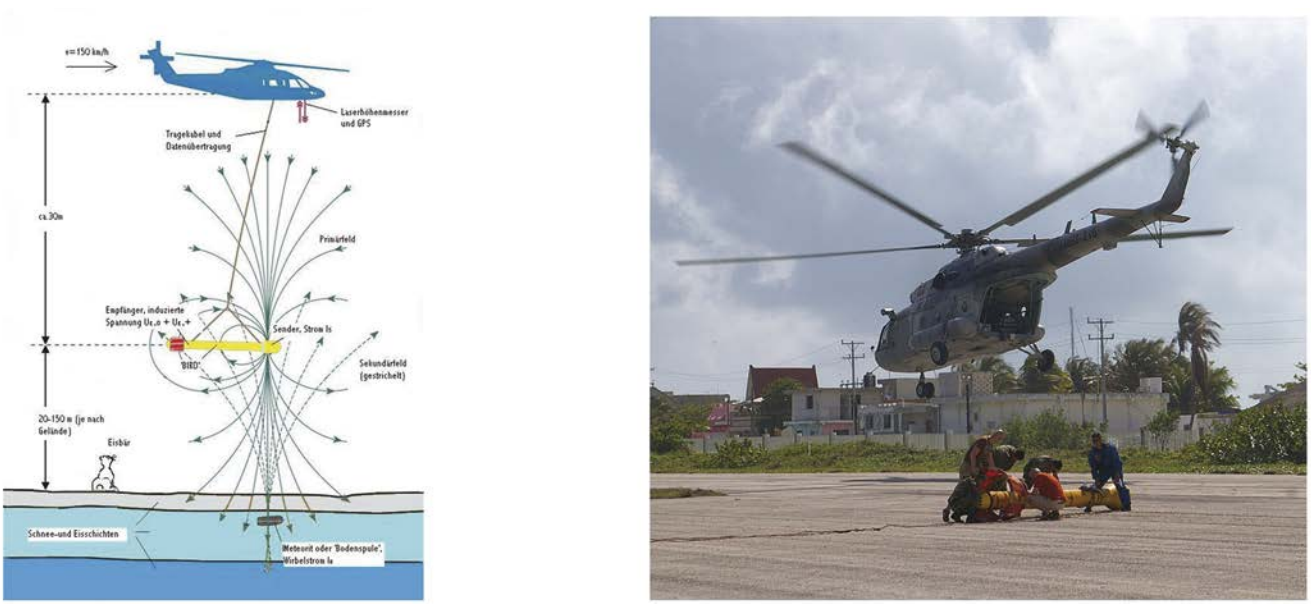

Figure 3: Left: principle of AEM-measurement method. Right: Navy helicopter with 'bird' on the Isla Mujeres, Cancun.
Figura 3. *Izquierda: principio del método de medición AEM. Derecha: helicóptero de la Marina con el 'bird' sobre la Isla Mujeres, Cancún.*

are governed by electromagnetically emitting hardware components built into the bird as dc-dc converters or ventilators, and by temperature. During the analysis, measurements of drift and noise, as well as system parameters such as temperature, geometry, humidity, air pressure and acceleration for crucial components have been carried out both on the ground and in flight. Temperature and pressure dependencies have been investigated in technical documentation and by laboratory measurements. Intermediate results showed a complex, mainly temperature governed behaviour of the system. A fitting system algorithm was programmed which is able to reproduce more than 90% of the drift amplitude by processing pure system temperature data of crucial circuit components (coils, capacitors, and resistors).Therefore, temperature changes, such as those caused by changes in flight altitude, speed (wind cooling), or shadowing (from helicopter or clouds), emerged as important drift sources. Different, but equally important sources are the heating of hardware components in the transmitter or computer section (Schiller *et al.,* 2010).

Data Processing

Based upon the findings of the comprehensive system analysis it was possible to derive new processing concepts and develop a set of standard and advanced processing procedures for improving the image of the hidden conduit system. In the case of the Tulum AEM survey the following processing procedures have been applied:

- General Gaussian noise reduction filter (standard).
- Q-coil scaling (standard).
- Reduction of linear drift by means of nulling data (standard).
- Damping of external active interferences (advanced).
- 'In-line nulling' - automatic drift estimation and correction by means of high altitude data (including correction of transmitter drift - advanced).
- 'Synthetic gradient method' - residual drift offset estimation by analysis of height correlation and correction (advanced).
- Semi-automatic data editing (standard).
- Enhancement of linear structures (advanced).
- Data inversion (standard).
- Background reduction in inversion results for enhancement of structural information (advanced).

The damping of externally in-coupled interferences (ringing coupled infrom radio transmitters, power lines, railway, etc.) is done by specific non-linear filtering of the in-phase and quadrature component of the signal which results in an effectively dampened interference amplitude. Another method is to analyse the phase shift between the in-phase and quadrature component. If the interference is actively coupled in or caused by internal resonant effects there is a specific phase shift which can be used as a filtering criterion.

The automatic drift correction works with two stages - 1) *In-line nulling*: if data is acquired above a certain altitude (e.g. 200 metres above ground in the case of Tulum) one can assume that no signal is sensed from underground, so the residual signal amplitude is caused by pure drift (this is also the idea of the conventional nulling-procedure at the beginning and end of a survey line, where the drift offset is nulled at approx. 1,000 feet above ground). Very often the topography is of the type that the high altitude limit is exceeded during measurement (e.g. above canyons) so that more points for more accurate drift estimation and correction can be used.

2) *Synthetic gradient method*: A way for refining the drift estimation is the analysis of signal/height correlations. It utilizes the fact that in general the raw signal exhibits a strong correlation to the measurement altitude due to its exponential decay with height. By extrapolating the height dependency of the signal data within a certain window to infinite altitude the residual offset, which represents the residual drift, is obtained. This technique assumes minimum data quality and some small scale lateral homogeneity of the electrical conductivity distribution in the underground.

After drift correction the data can be transformed to a constant height level above ground and be filtered. For enhancing linear structures a novel filtering technique has been developed in which a rotating linear weighted average filter is put on each point of the input image and outputs are calculated for 180 degrees angular range. The maximum output is then stored in a new image. The technique is sketched in Figure 7. This filter produces a map with superior signal-to-noise ratio and clearly visible lineament structures which indicate potential conduits (Figs.8, 9). However, the map contains no depth information which is extractible only through data inversion. Data inversion of frequency domain EM-data principally utilises the frequency dependent ground penetration (skin depth) of an electromagnetic field - the lower the frequency, the deeper the penetration depth. So each measurement (10 per second) is handled as an electromagnetic sounding based upon the four-frequency channel data. A 1-d layered earth model of the electric resistivity is calculated for each

measurement position. We used the software package UBC EM1DFM 1.0 developed at the University of British Columbia. In course of inversion, the electric resistivity for up to 25 layers with adjustable thickness was adapted to fit the AEM-data. The usual inversion result, i.e. the depth section beneath a survey line, shows minima and maxima of the electric conductivity distribution where peaks correlate with conduits but no distinct depth-defined structures are visible. Detailed analysis showed that large vertical gradients are dominating the inversion result which is caused by the strong secondary field originating in both the fresh- and salt-water body. Large gradients might hide weak signals containing important structural information. Consequently, this dominating background was modelled and subtracted from the initial inversion result to enhance hidden structural information.

Results

The developed two-stage automatic drift correction method is shown in Figures 4 and 5 by means of an example representing the four channel in-phase (left) and quadrature (right) data of three survey lines in one record. In Figure 4 the red curves are the raw signals, including drift, whilst the blue curves are the first stage drift corrected signals. Between the lines the helicopter changes to high altitude for nulling which is indicated by the two basins in the signal graphs where the signal from the ground drops to near zero. Here only the drift offset remains. After non-linear drift estimation and correction the basins coincided well with zero, so the drift was corrected in the first approach. Residual drift is corrected by the analysis of height correlations and shown in Figure 5. Red lines show the first stage drift corrected data and the blue lines show the final drift correction result. Negative artefacts are turned into positive signals, other amplitudes experience further adjustment.

This drift corrected data was then reviewed and corrected for residual artefacts where necessary, transformed to constant height above ground, and mean reduced to get rid of stripping artefacts. This led to images as shown in Figure 6. In this example 7200 Hz channel data is shown. Linear structures are already visible but contaminated by noise. The application of

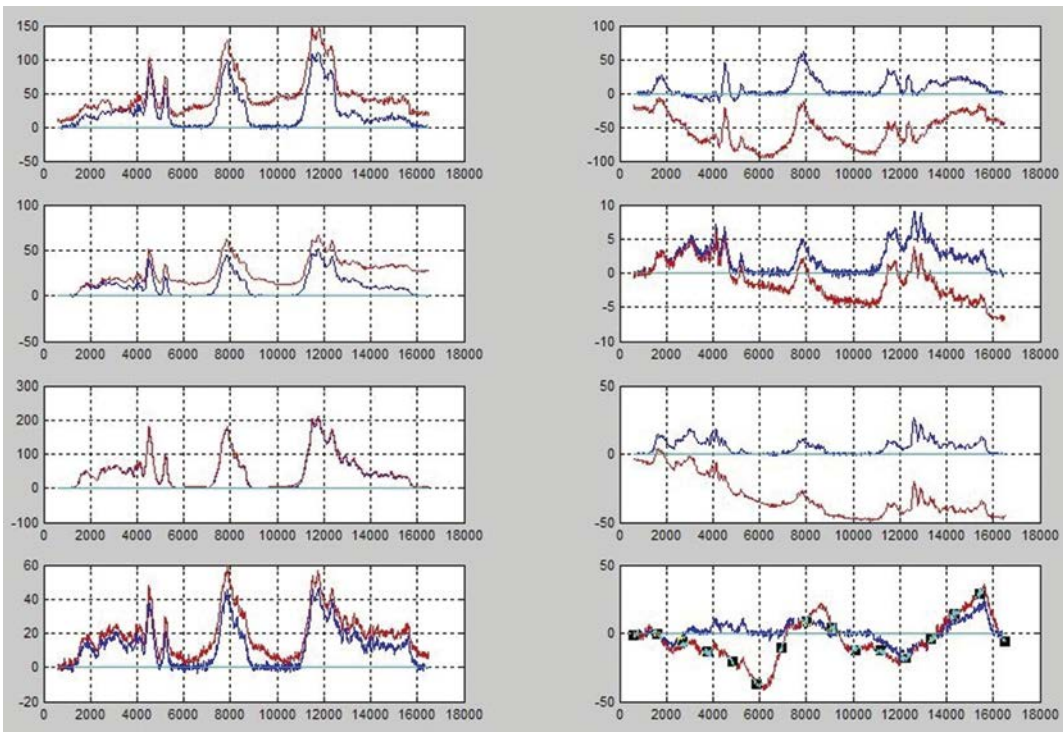

Figure 4: Automatic drift correction - first stage, using high altitude data. Frequency channels 1-4 (top to bottom), left: in-phase, right: quadrature. Red: raw signal. Blue: drift corrected. Vertical axis: ppm, horizontal axis: metres.
Figura 4. *Corrección automática de la deriva - primera etapa, utilizando datos de altitud. Canales de frecuencia 1-4 (de arriba a abajo), izquierda: en fase, derecha: cuadratura. Rojo: señal bruta. Azul: corregida para la deriva. Eje vertical: ppm, eje horizontal: metros.*

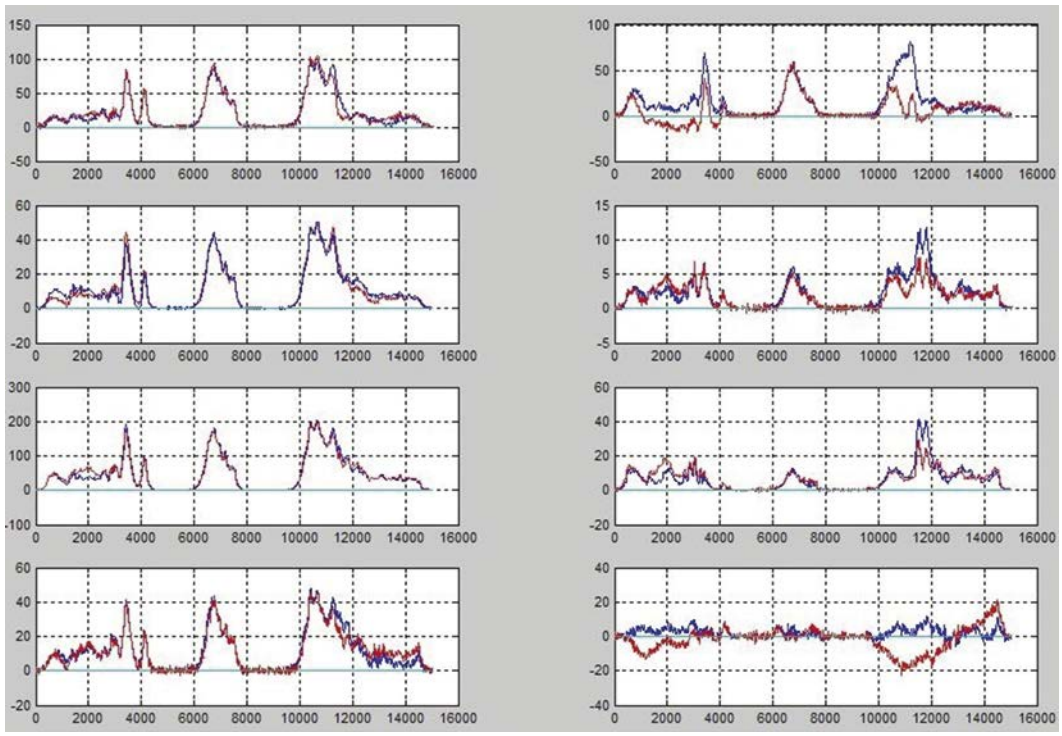

Figure 5: Automatic residual drift correction – second stage using height correlation. Red: first stage corrected. Blue: residual drift corrected. Vertical axis: ppm, horizontal axis: metres.
Figura. 5*. Corrección automática de la deriva residual – segunda etapa mediante correlación de altura. Rojo: primera etapa corregida. Azul: corregida para la deriva residual. Eje vertical: ppm, eje horizontal: metros.*

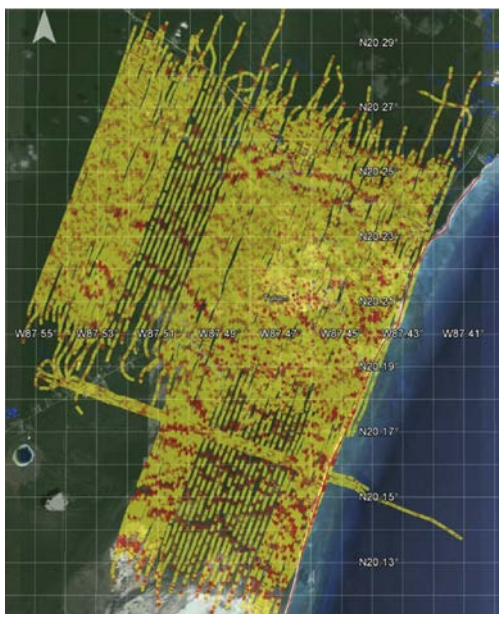

Figure 6: 7200 Hz channel of 2007 and 2008 surveys after drift correction, height reduction and destripping (Google Earth © map with overlay).
Figura 6*. Prospección de 2007 y 2008, en el canal de 7200 Hz, después de corrección de deriva, reducción de altura y "destripping" (mapa © de Google Earth con recubrimiento).*

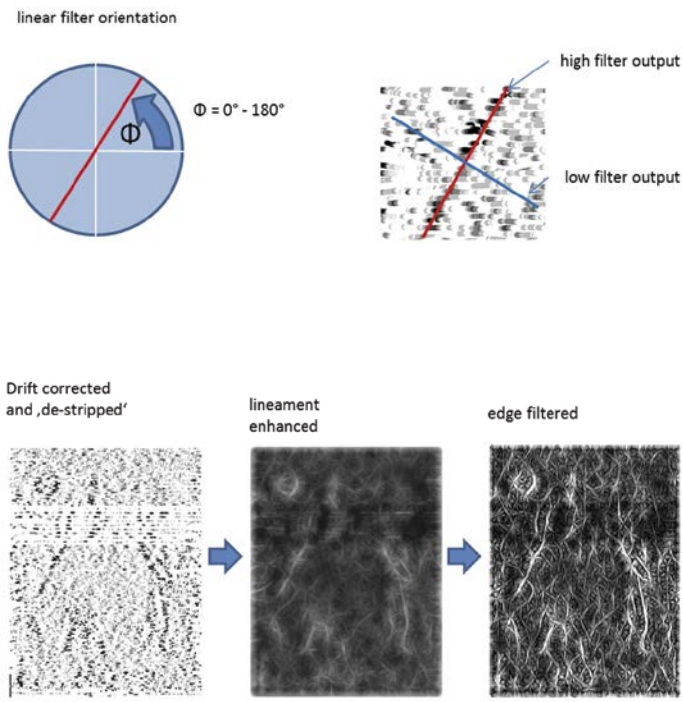

Figure 7: Principle of the rotational lineament enhancement filtering.
Figura 7*. Principio del filtro rotacional de realce de lineamientos.*

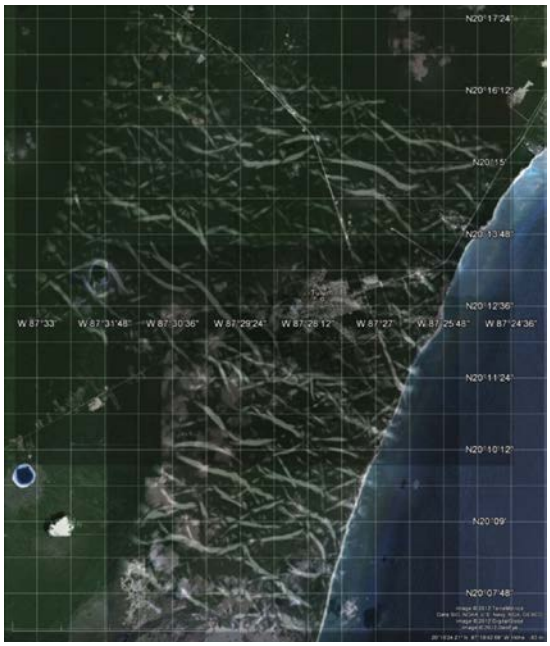

Figure 8: Data as shown in Figure 5 after rotational lineament enhancement filtering (Google Earth © map with overlay).
Figura 8*. Datos mostrados en la Fig. 5 después del realce de lineamientos por filtro rotacional. (© mapa de Google Earth con recubrimiento).*

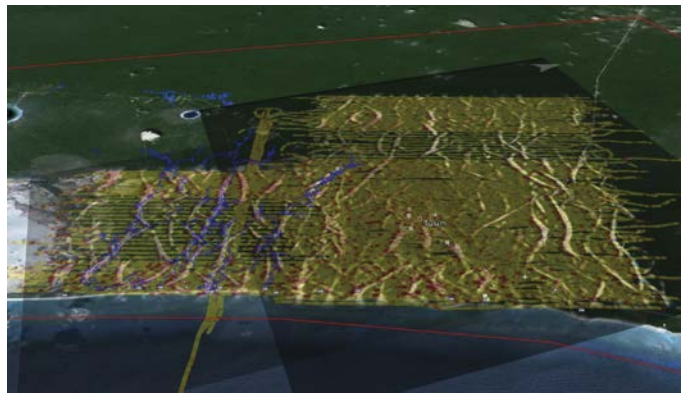

Figure 9: Figures 6 and 8 combine the overlay of cave survey data of the Ox Bel Ha and Ich Tunich systems (Google Earth © map with overlay).
Figura 9*. Combinación de las figuras 6 y 8 por superposición de los datos recopilados en los sistemas de cuevas Ox Bel Ha y Ich Tunich (© mapa de Google Earth con recubrimiento).*

the rotating filter techniques as sketched in Figure 7 leads to a map as shown in Figures 8 and 9. Here, a number of linear features have been enhanced which were not recognised in the noisy input data. This result represents a kind of propability distribution for underground conduits.

After a quick review and residual editing the automatically drift reduced AEM-data was inverted for the distribution of apparent electrical conductivity with the standard method. The background reduction of the strong gradient field the inversion result was then conducted.

Both are shown in Figures 10 and 11 by means of another example which is the inversion of a record comprising three lines ofsome 45 kilometers total length. The maximum depth of inversion is 38 meters equal to the modelled 19 layers of two-metre thickness each. The colours correspond to a logarithmic scale derived from the apparent electrical conductivity which was introduced to account for the large dynamics.

Figure 10 shows the standard inversion result (top), the derived gradient field (middle), and the residual conductivity distribution (bottom). Due to the very different scales the structures are laterally extremely compressed and not interpretable.

Figure 11 shows the same information as in Figure 10 - bottom but laterally expanded to a near realistic

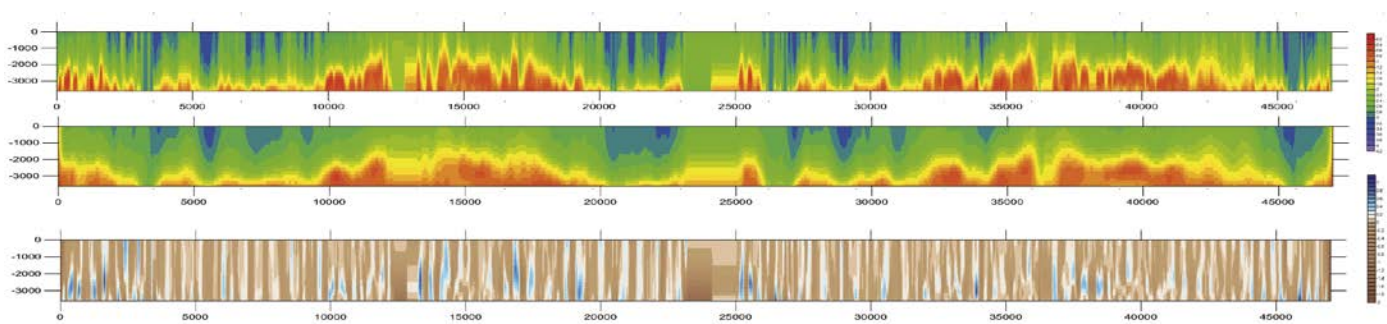

Figure 10: AEM record YUL046 - four lines in one record, 45 km total length. Top: result of standard inversion, layered half -space model - 19 layers of 2 metres each. Middle: model of gradient field. Bottom: residual field. Log10 of electrical conductivity, depth labels in centimetres.
Figura 10*. Registro YUL046 de la prospección AEM- cuatro líneas en un registro, 45 km de lontigud total. Parte superior: resultado de la inversión estándar, modelo de capas - 19 capas de 2 metros cada uno. Parte media: modelo de campo de gradientes. Parte inferior: campo residual. Logaritmo decimal de la conductividad eléctrica, etiquetas de profundidad en centímetros.*

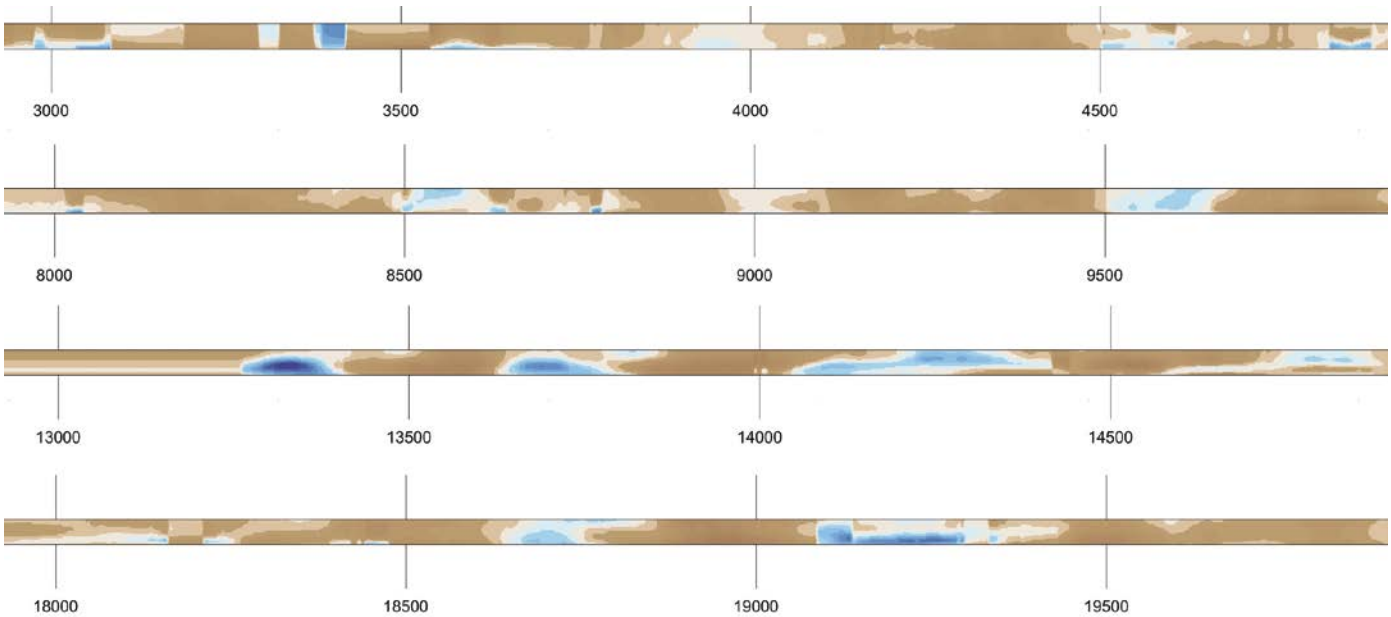

Figure 11: Examples of expanded depth sections of the residual field in Figure 10, length marks in metres, up to 38 metres depth.
Figura 11. *Ejemplos de secciones de mayor profundidad del campo residual de la figura 10, marcas de longitud en metros, se extienden hasta 38 metros de profundidad.*

ratio of horizontal to vertical scale. Here structures are recognized. The big artefacts at profile 3,000-3,500, 13,000 and 14,500 metres are caused by dummy data. Smaller artefacts come from instabilities of the first frequency channel. The colour coding indicates positive conductivity anomalies as bluish and negative ones as brownish which should give an intuitive picture of potential conduits hidden in the limestone. Figure 12 shows several depth sections combined with the enhanced map and cave survey data.

Discussion

The developed automatic drift reduction is time saving, more accurate and also considers variations of the transmitter field which is sensed with a pick-up coil. In surveys where the topography is more varying than in the case of Tulum many 'in-line' measurements above a certain altitude limit can be used for 'in-line' estimation of the drift. AEM-nulling could be skipped, which would save a lot of time and fuel. The synthetic gradient method is the only one capable of giving objective drift offset estimation, even during low-level flights. Whilst the automatic drift correction of one line is a matter of seconds, a quick review and occasional residual editing of the data should be retained as good practice. All together, the data pre-processing is more consistent and accelerated to a factor of five to ten. Data which was not interpretable so far can be kept; misinterpretation due to artefacts is less likely. The rotating filter technique significantly improves the signal-to-noise ratio and yields a very good lateral definition of structures. The generated map shows a very complex network of smaller and larger potential conduits, which correlate well with

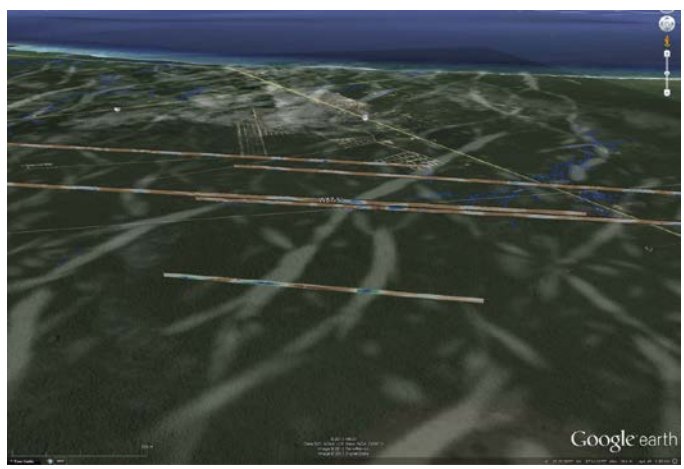

Figure 12: Enhanced AEM-map combined with depth sections and cave survey data. Viewed from inland eastwards, with the town of Tulum upper middle (Google Earth © map with overlay).
Figura 12. *Mapa AEM mejorado y combinado con secciones profundas y datos de exploración de la cueva. Mirando desde el interior hacia el este con el pueblo de Tulum en la parte media superior (mapa de Google Earth © con el recubrimiento).*

the cave systems already explored. The interpretation has to take into account anomalies caused by roads or power lines or other factors related to civilization. The result is a pure 2d-map without depth information. Nevertheless, this data provides a signifiantly improved input to both advanced hydrologic modelling and the decision making processes.

Background reduction in the standard inversion results yielded the best readable lateral and depth information of karst structures scanned by AEM so far. It effectively suppresses the dominating effect of the salt-water body. Features found in the enhanced sections are mostly well correlated with known conduits and are literally deepening the picture. In this study the inversion depth was generally limited to 36 or 40 metres, since the underlying salt-water body reduces the penetration depth of the system. Figure 9 shows a combination of survey data, an enhanced map and vertical sections derived from the AEM measurements. Consequent regular scanning principially enables the compilation of a 3d-map of the conduit system, which is currently in progress. The method is a pure linear transformation and does not generate artificial information which is not contained in the standard inversion results. The approach is at a preliminary stage and further different background modelling techniques will be tested in the near future to also extract high resolution information on the groundwater table and the halocline surface.

Conclusions

Aerogeophysics combined with advanced data processing can provide significant advantages for hydrological studies. The method is capable of rapidly delivering crucial structural information on karst-water regimes in areas of difficult accessiblity and with unique depth resolution down to depths of 30 to 60 metres, depending on the general electrical conductivity distribution in the subsurface. Whilst the context of this study especially addresses the potential impact of the on-going urbanization of Tulum for its special karst-water resource, the methods developed and applied would also form important contributions in similar groundwater studies and in more complex environments such as those found, for example, in the Mediterranean region.

Acknowledgements

We thank the Amigos de Sian Ka'an, Robert and Richard Schmittner (Xibalba Diving Center), Bil Phillips (Speleotech), Simon Richards for their great support, and we are grateful to the Austrian Science Fund which financed the projects HIRISK (L354-N10), XPLORE (L524-N10) and XIBALBA (I994-N29), the Austrian Academy of Sciences for further financial support (programme 'Man and Biosphere') and the Geological Survey of Austria.

References

Bauer-Gottwein, P. et al. 2011. Review: The Yucatán Peninsula karst aquifer, Mexico. *Hydrogeology Journal*, 19(3), 507-524.

Beddows, P.A. 2004. *Groundwater hydrology of a coastal conduit carbonate aquifer: Carribean coast of the Yucatán Peninsula, México.* PhD Thesis, University of Bristol, Bristol, 303 pp.

Gondwe, B.R.N., 2010. *Exploration, modelling and management of groundwater-dependent ecosystems in karst – the Sian Ka'an case study, Yucatan, Mexico*. PhD Thesis, Technical University of Denmark, Kongens Lyngby, 86 pp.

Gondwe, B.R.N. et al., 2010. Hydrogeology of the south-eastern Yucatan Peninsula: New insights from water level measurements, geochemistry, geophysics and remote sensing. *Journal of Hydrology*, 389(1-2), 1-17.

Motschka, K. 2001. Aerogeophysics in Austria. Bulletin of the Geological Survey of Japan 52(2/3):83–88.

Ottowitz, D., 2009. *3D-Modellrechnung der Karststrukturen des Ox Bel Ha Höhlensystems zur Methodenevaluierung– Aeroelektromagnetik*. MSc Thesis, University of Vienna, Austria, 123 pp.

Reynolds, J. M. 1997, *An Introduction to Applied and Environmental Geophysics*, John Wiley & Sons Inc.

Schiller, A., Klune, K., and Schattauer, I. 2010. Advanced AEM by comprehensive analysis and modelling of system drift. EGU General Assembly 2010, *Geophysical Research Abstracts*, Vol.12 EGU2010-11995-1.

Schiller, A., Supper, R., Vuilleumiere, C., Ottowitz, D., Ahl, A., and Motschka, K. 2012. *Airborne and ground geophysics for modelling a karstic conduit system: New results from the 2007-2011 campaigns in Tulum.* Near Surface Geoscience 2012, Remote Sensing Workshop, Proceedings of the 18th European Meeting of Environmental and Engineering Geophysics, Paris.

Schiller, A., Supper, R., Merediz Alonso, G., Ottowitz, D., Vuilleumiere, C., Motschka, K. 2013. *Aero-electromagnetic mapping of the hidden ground water conduit systems beneath the Tulum Karst plains.* IAGA, 12th Scientific Assembly, Merida, August 26-31, 2013, abstracts 1.3-7, abstract volume p. 102.

Supper, R., Motschka, K., Ahl, A., Ottowitz, D., Bauer, P., Gondwe, B., Merediz Alonso, G., Römer, A., Kinzelbach, W. 2009. Spatial mapping of submerged cave systems by means of airborne electromagnetics: an emerging technology to support protection of endangered karst

aquifers. Near Surface *Geophysics*, Special Issue on Hydrogeophysics – Methods and Processes, 7 (5-6), 613-627.

Supper, R., Schiller, A., Jochum, B., Ottowitz D. 2010. *Geophysikalische Messungen in Tulum (Mexiko)* – 2010, Österreichische Akademie der Wissenschaften, doi:10.1553/mab-geophys-tulum-2010.

Vuilleumier, C. 2011. *Stochastic modeling of the karstic system of the region of Tulum (Quintana Roo, Mexico)*, MSc Thesis, University of Neuchâtel (Switzerland), 37 pp.

Recibido: febrero 2015
Revisado: abril 2015
Aceptado: mayo 2015
Publicado: marzo 2016